FTIR Method for VLE Measurements of Acid-Gas–Alkanolamine Systems

William J. Rogers, Jerry A. Bullin, Richard R. Davison, Richard E. Frazier, and Kenneth N. Marsh
Chemical Engineering Dept., Texas A&M University, College Station, TX 77843

The standard industrial process for the purification of natural gas is to remove acid gases, mainly hydrogen sulfide and carbon dioxide, by the absorption and reaction of these gases with alkanolamines, but the lack of reliable and accurate vapor-liquid equilibrium (VLE) data impedes the commercial application of more efficient alkanolamine systems. The objective of this research was to develop an FTIR apparatus and an in-situ technique capable of making VLE measurements of acid-gas–aqueous alkanolamine systems and to improve the accuracy of vapor–liquid equilibrium measurements at low hydrogen sulfide and carbon dioxide concentrations. The new FTIR apparatus and technique were tested in VLE measurements of low concentrations of carbon dioxide and hydrogen sulfide in aqueous mixtures of diethanolamine.

Introduction

The standard process for removal of acid gases such as hydrogen sulfide and carbon dioxide from natural, process, and synthetic gas is by absorption and reaction of these gases with aqueous alkanolamine solutions.

Accurate and reliable vapor–liquid equilibrium (VLE) data are critically needed to use and develop more energy-efficient amine systems for this purification process. To help provide the data needed for these models, a novel method for the measurement of acid-gas and sulfur gas–amine VLE systems was developed. This unique technique uses a Fourier transform infrared (FTIR) spectrometer to measure gas pressures and loading in amine solutions. One feature of this new method is to measure species concentration without removal of sample from the VLE system.

An important objective of this research is to improve the accuracy of VLE measurements of amine systems at low concentrations of sulfur compounds. This FTIR method is suitable for acid gases such as carbon dioxide (CO_2), and for sulfur-containing gases including hydrogen sulfide (H_2S), carbonyl sulfide (COS), carbon disulfide (CS_2), and mercaptans and for amines including diethanolamine (DEA), methyldiethanolamine (MDEA), monoethanolamine (MEA), diglycolamine (DGA), and mixed amine systems.

This article reports the application of the new FTIR method to measurements of carbon dioxide and hydrogen sulfide in aqueous solutions of DEA. For the process of removing acid gases, MEA and DEA are the most used of the alkanolamines because of their high reactivity, ease of regeneration, low hydrocarbon absorption, and low cost (Issacs et al., 1980). DEA and MEA have a similar carbon dioxide absorption capacity (Sartori and Savage, 1983). Compared with MEA, DEA is more stable thermally and has a lower enthalpy of reaction (Davis et al., 1993) and a lower volatility (Stewart and Lanning, 1994).

This research uses an FTIR method to analyze the equilibrium concentrations of vapor and liquid phases in sulfur and acid-gas–alkanolamine systems. The sulfur compounds and carbon dioxide in these systems absorb radiation in the mid-infrared (IR) frequency range and can be detected by FTIR spectroscopy. Each component absorbs IR energy with a unique spectrum that results from its molecular structure. This characteristic spectrum is measured during experiments and can be used to identify a component and to measure its concentration.

Featured in this FTIR method is a closed VLE system in which both vapor and liquid phases are measured without removal of samples. This design permits measurements without disturbing the system equilibrium. Sulfur compounds are strongly adsorbing on surfaces, and methods that require external sampling are subject to shifts in composition caused by unequilibrated surfaces. Adsorption losses during sampling and analysis increase significantly as the acid-gas concentration decreases. In this closed system, however, the sample is equilibrated with all surfaces.

Correspondence concerning this article should be addressed to J. A. Bullin.

This work demonstrates the feasibility of FTIR measurements of VLE systems of acid gases in aqueous solutions of alkanolamines. Measurements were made of aqueous systems of DEA together with various concentrations of carbon dioxide and hydrogen sulfide near 323 and 313 K. Carbon dioxide was measured in all systems either as an added or as a residual component.

Apparatus and Experimental Method

Apparatus

The apparatus consists of a Nicolet 60SX FTIR spectrometer and a VLE apparatus. The Nicolet spectrometer was optically coupled to the VLE apparatus using mirrors for directing the IR beam to the VLE apparatus and for directing the returning IR beam to the IR detector. Additional mirrors were installed to direct the IR beam to each of three IR measurement cells and to the IR detector. To remove extraneous carbon dioxide and water vapor, the path of the IR beam was enclosed and purged with high-purity ($\geq 99.99\%$) nitrogen vapor at a flow rate of ~ 157 std. cm^3/s.

The VLE apparatus, showing the FTIR spectrometer coupling with the IR measurement cells, is shown in Figure 1. Apparatus construction materials were selected to be stable with contact with acid gases, such as stainless steel 316 or Hastelloy. Additional apparatus construction details are discussed by Frazier (1993).

The sample was mixed by circulating the liquid and vapor from the VLE cell, with total volume of ~ 1 L and sample liquid depth of ~ 7–8 cm, through IR measurement cells and back to the VLE cell. Because vapor components vary in their IR absorbance efficiency, two vapor cells for IR measurement were used with windows of ZnSe and BaF_2. A short cell with ~ 0.64-L volume and 0.14-m pathlength was used for strongly absorbing components, such as carbon dioxide, and a long cell with ~ 35 L-volume and 73-m pathlength was used for weakly absorbing components, such as hydrogen sulfide.

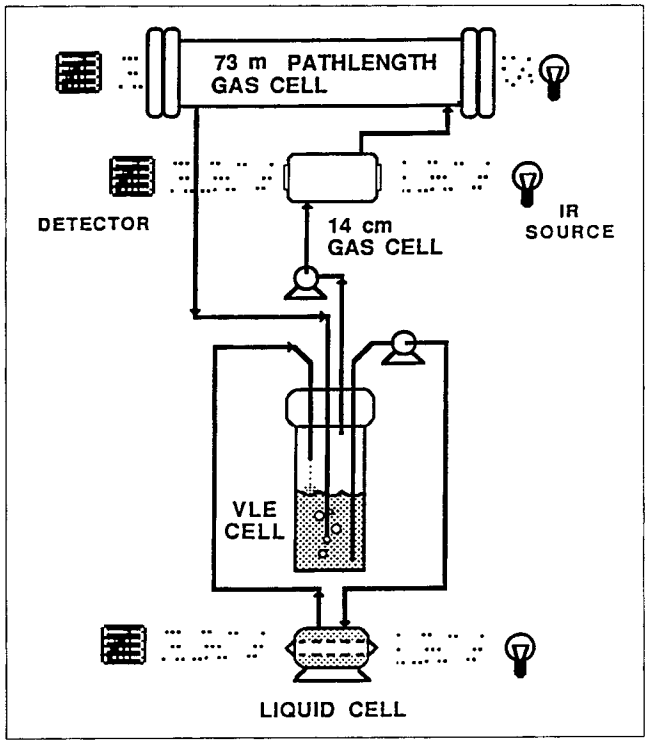

Figure 1. FTIR and VLE apparatus.

The long cell together with an internal assembly of five mirrors were fabricated at Texas A&M University following an optical design by White (1942). The 73-m pathlength of this cell is greater than its physical length (~ 2 m) through 36 reflections of the IR beam between the mirrors positioned near each end of the cell. Each mirror has a reflective layer of gold with a silicon oxide coating. Hydrogen sulfide reacts very slowly with gold below 100°C, and the oxide coating provides additional protection while only slightly reducing the energy of the traversing IR beam.

Because liquid water is highly absorbing of IR energy, the liquid measurement cell features a cylindrical internal-reflectance (CIR) method for sampling. A Spectra-Tech CIR cell contains a cylindrical ZnSe crystal, 8 cm long $\times$ 0.63 cm dia., which reflects a focused IR beam in transit through the cell.

The vapor measurement cells and vapor sample circulation lines were controlled to a temperature well above the VLE cell temperature to prevent water condensation. The CIR cell temperature was controlled at a value below the VLE cell temperature to prevent vapor from forming in the liquid circulation line. As the circulating vapor and liquid reentered the VLE cell, the vapor and liquid were each controlled at the temperature of the VLE cell.

Sample temperatures within the VLE cell were measured with an Omega platinum resistance thermometer (PRT), which was calibrated to within 0.005 K against a PRT with a known calibration traceable to the National Institute of Standards and Technology (NIST). Pressures were measured with a Druck absolute-pressure transducer with a silicon-crystal-bonded diaphragm of Hastelloy. The transducer, controlled at 343 K, was calibrated to within 0.02% of pressures from vacuum to 110 kPa against a Paroscientific quartz pressure transducer with a calibration traceable to NIST. The VLE cell was inside a stirred ethylene glycol bath and was controlled during experiments to within ~ 0.02 K.

Total pressure measurements were made with the pressure transducer on the vapor circulation line that connected the VLE cell to the sample measurement cells. Small pressure gradients generated by the vapor pumping were identified by pressure measurements at various positions on the vapor circulation line. These pressure gradients were unimportant, because sample calibrations were performed under approximately the same conditions as the sample measurements in typical experiments. As a result, the sample spectral areas corrected to a total pressure of 103.4 kPa were unaffected by these gradients.

A Metal Bellows pump with a stainless steel bellows and check valves circulated the sample vapor, and a Micropump positive-displacement pump circulated the sample liquid. Vapor flow was measured by a sight glass flowmeter with a needle-valve flow regulator. Liquid flow rate was measured with a sight glass flowmeter and controlled by varying the displaced volume rate of the Micropump liquid pump.

Experimental method

During an experiment, sample vapor was introduced into the apparatus and mixed with a nitrogen diluent used to maintain the total pressure between 96 and 110 kPa. While

circulating, the sample also equilibrated with the cell and tubing surfaces. Following mixing, the spectra of the sample vapor were measured to determine the amount of sample vapor added. The vapor was then mixed with an aqueous alkanolamine sample in the VLE cell at constant temperature.

The mixing of sample vapor and liquid was accomplished by bubbling the vapor through the liquid (at a depth of ~ 3.5 cm) at the rate of 33–50 cm^3/s, and simultaneous circulation of the liquid through the liquid IR measurement cell and back to the VLE cell at the rate of 0.17–0.33 cm^3/s. After the vapor and liquid were mixed and allowed to equilibrate, spectra measurements were made on the vapor and liquid in the IR measurement cells. The vapor measurements following mixing were compared with those before mixing to determine the amounts of sample added to the liquid.

Equilibrium mixing times of the vapor and liquid, 3.2×10^4–3.6×10^4 s, depended on the vapor and liquid flow rates and estimated by repeated spectra measurements. Samples were mixed longer than was found necessary for system equilibrium as tested by repeated measurements. Following VLE measurements, additional sample vapor was added to the system to produce another VLE composition for measurement.

With every measurement of carbon dioxide in the short vapor cell, a measurement of carbon dioxide was made along an IR beam path that bypassed the cell to determine the contribution of the background carbon dioxide to the total spectrum area. The sample measurement was then corrected for the background carbon dioxide using background carbon dioxide calibration data. Carbon dioxide was measured by integrating its spectrum over the frequency range of 2,283 to 2,390 cm^{-1}. Spectra of carbon dioxide are shown in Figure 2.

Hydrogen sulfide was measured in the long vapor cell and required no background hydrogen sulfide correction. There are small overlaps of the water, amine, and hydrogen sulfide spectral regions, but the water and amine vapor spectra were removed from hydrogen sulfide spectra by signal ratioing. A spectrum of the sample vapor without added hydrogen sulfide was used in each system as a reference to determine the hydrogen sulfide absorbance spectra. Hydrogen sulfide measurements were made by integrating its spectrum over the frequency range of 2,394 to 2,578 cm^{-1}. In the presence of high concentrations of carbon dioxide, the frequency range of hydrogen sulfide measurement was decreased to 2,426 to 2,578 cm^{-1}. Spectra of hydrogen sulfide are in Figure 3.

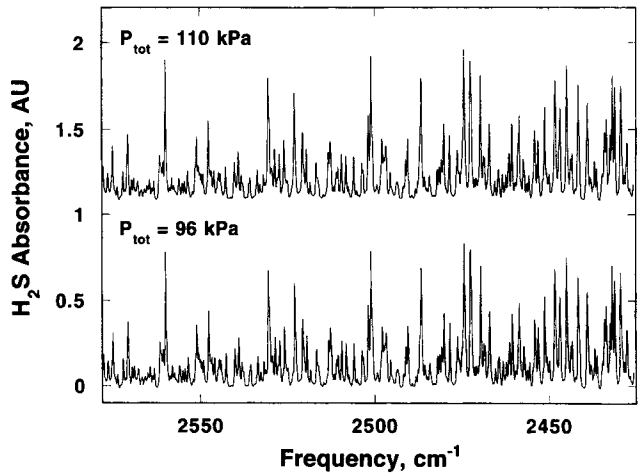

Figure 3. Hydrogen sulfide vapor spectra.

Liquid species were measured in the CIR liquid cell. A spectrum of carbon dioxide species in aqueous DEA with a measurement frequency range of 1,388 to 1,443 cm^{-1} is shown in Figure 4, and a spectrum of hydrogen sulfide species in aqueous DEA with a measurement frequency range of 1,045 to 1,092 cm^{-1} is shown in Figure 5. A spectrum of the aqueous amine sample without added carbon dioxide or hydrogen sulfide was used as a reference to determine liquid species absorbance spectra. Residual carbon dioxide loading was determined using the solubility data at the lowest concentrations and the linear dependence of the carbon dioxide pressure with the loading function $Fn(CO_2)$, which is discussed below.

Calibration

Known pressures of hydrogen sulfide were measured at various total pressures from 96 to 110 kPa and fixed temperature with nitrogen as a diluent. Each amount of hydrogen sulfide was added and allowed to equilibrate with surfaces. When the hydrogen sulfide pressure stabilized, the pressure

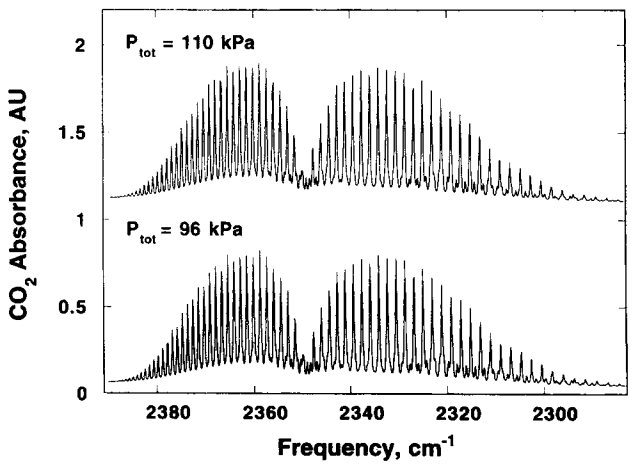

Figure 2. Carbon dioxide vapor spectra.

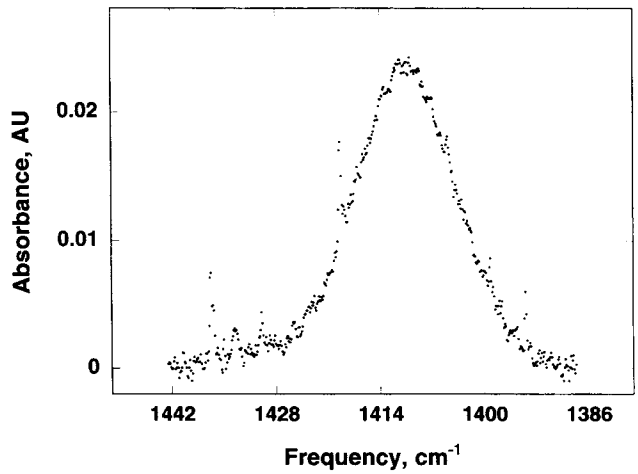

Figure 4. Carbon dioxide species in aqueous DEA.

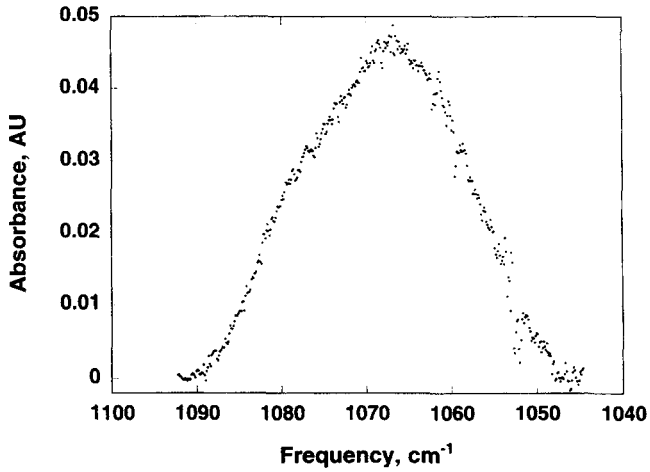

Figure 5. Hydrogen sulfide species in aqueous DEA.

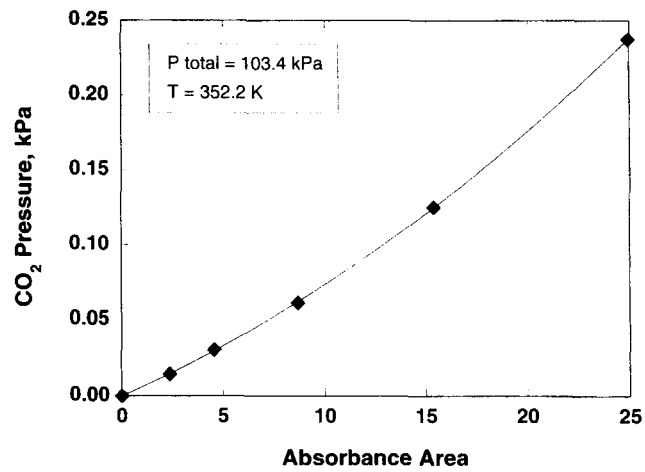

Figure 7. Carbon dioxide low-pressure calibration.

was recorded and nitrogen was then added for a total pressure of 96 to 110 kPa and then mixed prior to the calibration measurements. During these measurements, IR frequency regions for hydrogen sulfide were selected, and their spectral areas were calibrated from zero to 10.3 kPa hydrogen sulfide. Below 0.7 kPa, the hydrogen sulfide pressures are linear with absorbance area. A calibration curve for low-pressure hydrogen sulfide is shown in Figure 6. The dependence at higher pressures is progressively nonlinear but well behaved and reproducible.

Similar calibration measurements were made for carbon dioxide from near zero to 5.5 kPa. The carbon dioxide pressures are quadratic and well behaved with the spectral areas over this entire pressure range. A calibration curve for low-pressure carbon dioxide is shown in Figure 7. Calibration of background carbon dioxide was performed by measuring the carbon dioxide along an IR beam path that bypassed the short vapor cell by means of adjustable mirrors.

Spectra are affected by molecular interactions, which is a function of total pressure, as discussed by Thorne (1988, p. 280). Because of pressure broadening of spectra, vapor calibrations for ranges of partial pressures were conducted at total pressures from 96 to 110 kPa, using nitrogen as a diluent, to determine the dependence of spectral area on total pressure. Figures 2 and 3 display spectra for carbon dioxide and hydrogen sulfide at 96 to 110 kPa, the lower and upper total pressures for the calibrations and experiments. For a partial pressure of 0.125 kPa, the carbon dioxide spectrum over the measurement frequency range shown exhibits an increase in area of about 5% at the higher pressure. For a partial pressure of 5.51 kPa, the hydrogen sulfide spectrum over the measurement frequency range shown exhibits an increase in area of about 1.3% at the higher pressure. During experiments, spectral area measurements made at total pressures between 96 and 110 kPa were corrected for total pressure to 103.4 kPa (15 psia) using the calibration data. Experimental spectra areas were measured in the same manner as in the calibrations and over the same frequency ranges.

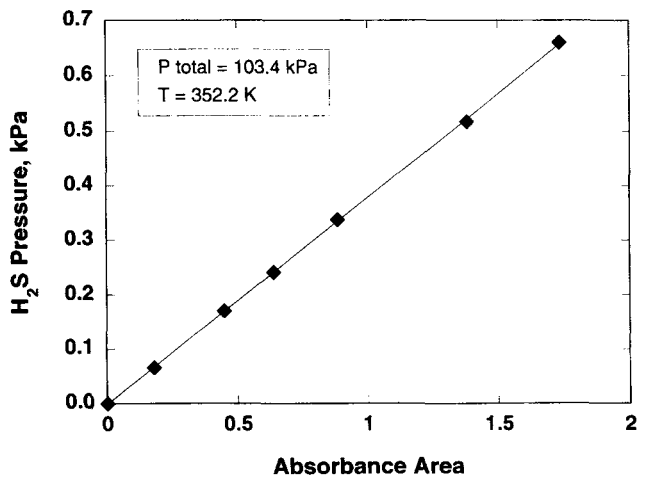

Figure 6. Hydrogen sulfide low-pressure calibration.

Liquid sample calibrations were performed by determining amounts of pure vapor absorbed by the liquid and measuring the corresponding spectral areas of the liquid sample. The amounts of vapor absorbed by the liquid were determined first through gas chromatographic (GC) measurement using gravimetrically prepared calibration samples and later by measurement of sample cell volumes. Liquid sample concentrations were checked by gas GC analysis of 0.001 cm^3 samples using TCD detection.

Reference spectra were made of each aqueous sample of DEA, which had been vacuum distilled to remove other alkanolamines and carbon dioxide, before any carbon dioxide or hydrogen sulfide was added. Reference spectra were made of the vapor of each DEA sample before carbon dioxide or hydrogen sulfide was added. These reference spectra were used as background in the analysis of sample spectra following each addition of carbon dioxide or hydrogen sulfide.

Uncertainties

Temperature of the measurement cells was controlled and measured to ± 0.1 K. Temperature of the VLE sample cell was controlled to ± 0.02 K and accurate to ± 0.03 K.

Sample pressures were measured by the Druck transducer with a precision of ± 0.007 kPa and an accuracy of ± 0.02 kPa or 0.02% of full scale pressure of 103 kPa. Once calibrated, the FTIR spectrometer was capable of determining carbon dioxide pressures with a precision of 0.1 to 0.4 Pa.

Hydrogen sulfide pressure precision was 4 to 7 Pa, which approaches the low detection limit of about 4 Pa in this study.

DEA/H_2O concentrations are accurate to ± 0.05 wt.%.

Overall uncertainty in measured values of sample partial pressures is estimated to be generally $\pm 5\%$, and the loading values are estimated to be within $\pm 6\%$, except at the lowest concentrations, when uncertainties were limited by the low detection limits of carbon dioxide and hydrogen sulfide, as listed before.

Multiple measurements over time were made to ensure that the system was at equilibrium with respect to temperature, pressure, and amine gas loading. Multiple measurements were performed without loss of precision, because the sample equilibrium was not significantly disturbed by the analytical technique.

Samples

All DEA samples, supplied by Aldrich with a nominal 99% purity, were distilled under vacuum to remove impurities, including impurity alkanolamines and were checked for impurities by GC. Based on GC measurements, the estimated purity of the distilled samples for measurements was 99.9%.

Samples of C.P. grade hydrogen sulfide of nominal 99.5% purity were supplied by Matheson with lot analyses listing purities of 99.7–99.8%. Samples of Coleman Instrument grade carbon dioxide with 99.99% purity were supplied by Matheson. Trigas supplied UHP nitrogen with 99.999% purity. The samples of hydrogen sulfide, carbon dioxide, and nitrogen were used without additional purification.

Equilibrium Reaction Model

Models of the equilibrium in the reactions of carbon dioxide and hydrogen sulfide with aqueous alkanolamine solutions can be used to relate the loading and pressures of the acid gases. These models can then be tested with experimental measurements of loading and partial pressure. At equilibrium, the sample partial pressure for carbon dioxide or hydrogen sulfide can be related to a liquid concentration of carbon dioxide or hydrogen sulfide at low concentrations by a limiting form of Henry's law, where the vapor fugacity coefficients are set to unity.

$$P_{CO_2} = H_{CO_2} \cdot [CO_2] \tag{1}$$

$$P_{H_2S} = H_{H_2S} \cdot [H_2S]. \tag{2}$$

Reactions of carbon dioxide and hydrogen sulfide in aqueous alkanolamine solutions are discussed by Austgen et al. (1989). As stated by Astarita and Savage (1982), the carbamate species, $(HO—CH_2—CH_2)_2—NCOO^-$, accounts for essentially all carbon dioxide loading at low concentrations in DEA, so a model of behavior at low loading can ignore the bicarbonate, HCO_3^- and its dissociation to carbonate, CO_3^{-2}. For hydrogen sulfide at low concentrations in DEA, the small dissociation of bisulfide, HS^-, to sulfide, S^{-2}, can be ignored. The important reactions for carbon dioxide and hydrogen sulfide in aqueous alkanolamine solutions at low concentrations are therefore

$$K_1 = \frac{[H_3O^+][OH^-]}{[H_2O]^2}, \qquad K_2 = \frac{[HCO_3^-][H_3O^+]}{[CO_2][H_2O]^2},$$

$$K_3 = \frac{[HS^-][H_3O^+]}{[H_2S][H_2O]}, \qquad K_4 = \frac{[A^0][HCO_3^-]}{[C^-][H_2O]},$$

$$K_5 = \frac{[A^0][H_3O^+]}{[A^+][H_2O]}. \tag{3}$$

Equations relating the dominant species in solution are therefore

$[A^0]$ = neutral amine concentration

$[A] = [A^0] + [A^+] + [C^-]$, total (prepared) amine concentration (4)

$[A^+] = [HCO_3^-] + [C^-] + [HS^-]$, charge balance, $[H_3O^+] \sim 0, [OH^-] \sim 0$ (5)

$\beta \cdot [A] = [C^-]$, CO_2 loading species at low concentration, $[HCO_3^-] \ll [C^-]$ (6)

$\alpha \cdot [A] = [HS^-]$, hydrogen sulfide loading species. (7)

The resulting VLE equations relating partial pressure and loading for low concentrations of CO_2 and H_2S in aqueous solutions of DEA are

$$P_{CO_2} = H_{CO_2} \cdot [CO_2] = H_{CO_2} \cdot (K_5 K_4 / K_2) \cdot \beta(\alpha + \beta)/(1 - \alpha - 2\beta)^2 \tag{8}$$

$$P_{CO_2} = H_{CO_2} \cdot (K_5 K_4 / K_2) \cdot \beta^2/(1-2\beta)^2, \quad \text{for only } CO_2 \text{ present, } \alpha = 0 \tag{9}$$

$$P_{H_2S} = H_{H_2S} \cdot [H_2S] = H_{H_2S} \cdot (K_5/K_3) \cdot [DEA] \cdot \alpha(\alpha + \beta)/(1 - \alpha - 2\beta) \tag{10}$$

$$P_{H_2S} = H_{H_2S} \cdot (K_5/K_3) \cdot [A] \cdot \alpha^2/(1 - \alpha), \quad \text{for only } H_2S \text{ present, } \beta = 0 \tag{11}$$

$$P_{CO_2}/P_{H_2S} = (H_{CO_2}/H_{H_2S}) \cdot (K_3 K_4 / K_2) \cdot (1/[DEA]) \cdot (\beta/\alpha) \cdot (1/(1 - \alpha - 2\beta)). \tag{12}$$

At the limit of low loading, Eq. 9 for carbon dioxide partial pressure, P_{CO_2}, reduces to the familiar dependence of the pressure on the square of the loading,

$$P_{CO_2} \sim \beta^2, \quad \text{or} \quad \log P_{CO_2} \sim \log \beta. \tag{13}$$

Likewise, in the limit of low loading at a given DEA concentration, Eq. 11 for hydrogen sulfide partial pressure, P_{H_2S}, reduces to a linear dependence of the pressure on the square of the loading,

$$P_{H_2S} \sim \alpha^2, \quad \text{or} \quad \log P_{H_2S} \sim \log \alpha. \tag{14}$$

For low concentrations of both carbon dioxide and hydrogen sulfide in DEA, the equations for partial pressure can be restated as follows:

$$P_{CO_2} \sim \beta(\alpha+\beta)/(1-\alpha-2\beta)^2 = \mathrm{Fn}(CO_2)_D \quad (15)$$

$$P_{H_2S} \sim [\mathrm{DEA}]\cdot\alpha(\alpha+\beta)/(1-\alpha-2\beta) = [\mathrm{DEA}]\cdot\mathrm{Fn}(H_2S)_D \quad (16)$$

$$P_{CO_2}/P_{H_2S} \sim (1/[\mathrm{DEA}])\cdot(\beta/\alpha)/(1-\alpha-2\beta) = (1/[\mathrm{DEA}])\cdot\mathrm{Fn}(CO_2, H_2S)_D, \quad (17)$$

where $\mathrm{Fn}(CO_2)_D$, $\mathrm{Fn}(H_2S)_D$, and $\mathrm{Fn}(CO_2,H_2S)_D$ are functions of the loading and represent the pressure or pressure ratio for a given DEA concentration, [DEA]. These relations are useful for representing VLE data in the limit of low concentrations of carbon dioxide and hydrogen sulfide in aqueous alkanolamines. The relations provide a linear relationship between sample pressure and loading function and predict that the sample pressure is 0 kPa in the limit of zero loading. In the discussion of experimental results, this reaction model was tested by VLE data using these limiting relations.

Note that this limiting model is not realistic at moderate to high concentration conditions, where activity coefficients deviate significantly from unity. Also, it is not realistic at high pH conditions, where hydroxide affects the equilibrium, which should apply for extreme low loading conditions (loading mole ratio < 0.002). Also, carbonate is neglected for simplicity even though it should contribute together with bicarbonate at extreme low loading and high pH conditions. Such high pH effects were not observed in our measurements.

Experimental Results

CO_2 in 20.2 wt. % DEA at 323.0 K

Measurements were made of fourteen mixtures of carbon dioxide in 20.2 wt. % DEA at 323.0 K. The solubility data are listed in Table 1 and are displayed in Figure 8 together with literature data by Murzin and Leites (1971) and Lee et al. (1974). These data are also displayed in Figure 9, which contains other carbon dioxide data reported here.

Carbon dioxide pressures below 0.008 kPa are shown to be linear with $\mathrm{Fn}(CO_2)_D$ in Figure 10 (Table 1) as predicted by the model of behavior at low concentrations discussed earlier. As was also predicted, the carbon dioxide pressure approaches 0 kPa, within the experimental error of ± 0.7 Pa in the pressure, as the loading approaches zero.

Table 1. CO_2 in 20.2 wt. % DEA at 323.0 K

P_{CO_2}/kPa	CO_2/DEA Mole Ratio
0.00034	0.00663
0.00055	0.00856
0.00054	0.00903
0.00062	0.00985
0.00090	0.01113
0.00145	0.01424
0.00365	0.02249
0.00563	0.02762
0.0104	0.03679
0.0186	0.05035
0.0432	0.07418
0.0947	0.1098
0.2035	0.1482
0.5515	0.2331

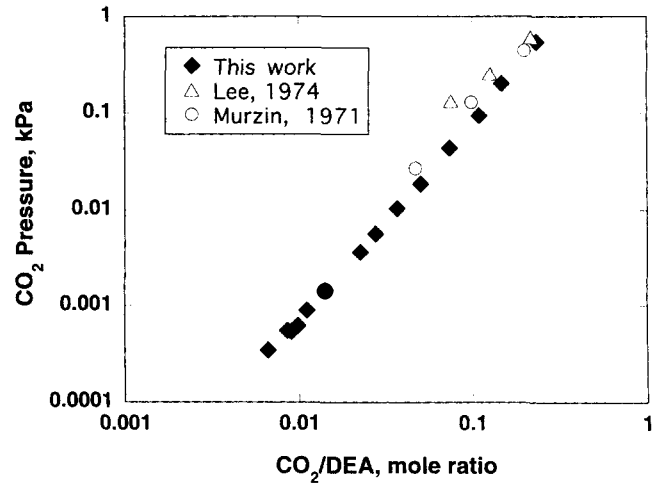

Figure 8. CO_2 solubility in 20.2 wt. % DEA at 323.0 K.

H_2S with $\beta \sim 0.0063$, in 20.3 wt. % DEA at 322.8 K

Four measurements were made of a VLE system with a small amount of added CO_2, which resulted in an initial loading, $\beta \sim 0.0063$, in 20.3 wt. % DEA at 322.8 K. Measurements were then made of five additional mixtures where the hydrogen sulfide was progressively added to the initial carbon dioxide loading. The data are listed in Table 2, and the solubility of hydrogen sulfide is shown in Figure 11.

Hydrogen sulfide pressures below 0.35 kPa are shown to be linear with $\mathrm{Fn}(H_2S)_D$ in Figure 12 (Table 2), and the hydrogen sulfide pressure approaches 0 kPa as the loading approaches zero, within the experimental error, as predicted by the model. The uncertainty of the two lowest hydrogen sulfide pressures in this experiment are within $\sim \pm 7$ Pa.

Carbon dioxide pressures below 0.007 kPa are shown to be linear with $\mathrm{Fn}(CO_2)_D$ in Figure 10 (Table 2) as predicted by the model. As the loading approaches zero, the carbon dioxide pressure approaches ~ 0.6 Pa, which is approximately the

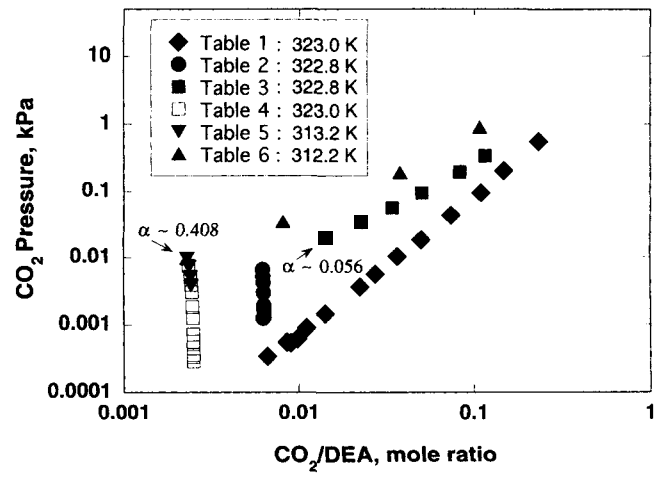

Figure 9. Carbon dioxide solubility in 20 wt. % DEA.

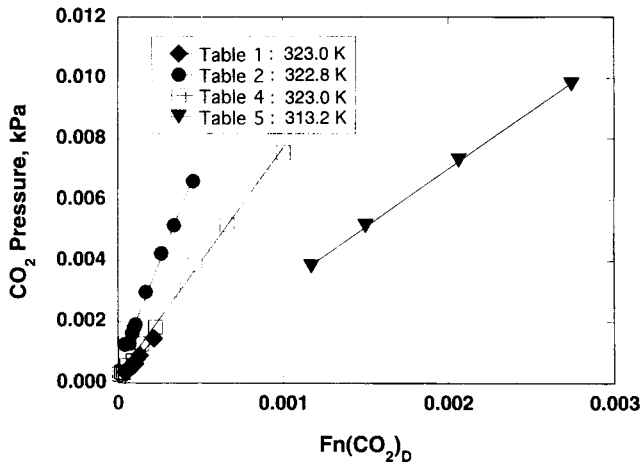

Figure 10. Low-pressure CO_2 in 20 wt. % DEA.

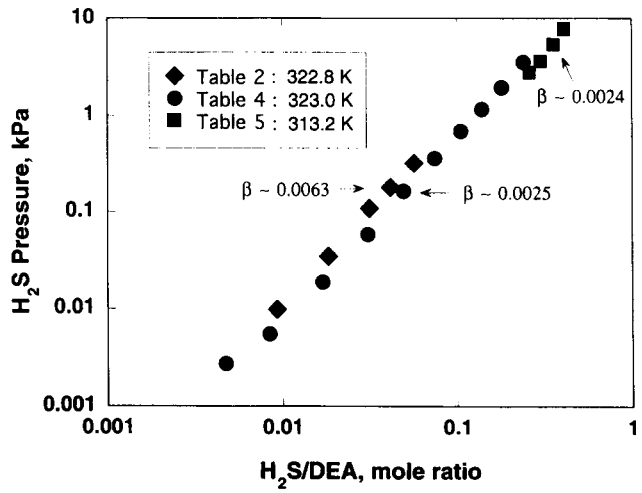

Figure 11. Hydrogen sulfide solubility in 20 wt. % DEA.

pressure uncertainty in this experiment. The ratio of carbon dioxide and hydrogen sulfide pressure, P_{CO_2}/P_{H_2S}, is plotted against $Fn(CO_2, H_2S)_D$ in Figure 13 (Table 2). The low concentration model predicts a linear rather than the quadratic dependence of the measured data shown here.

CO_2 with $\alpha \sim 0.056$ in 20.3 wt. % DEA at 322.8 K

Starting with an initial α, or $[H_2S]/[DEA]$, ~0.056, carbon dioxide was progressively added to 20.3 wt. % DEA at 322.8 K. VLE data from six measured compositions with added CO_2 are in Table 3, and the solubility of CO_2 in the DEA solution is in Figure 9 (Table 3), which shows the rise in CO_2 pressure and decrease in CO_2 loading as H_2S was added in the previous experiment (Table 2).

At carbon dioxide pressures of 0.06 kPa and below the pressure is linear with $Fn(CO_2)_D$ as predicted by the low concentration model. As the loading approaches zero, the carbon dioxide pressure approaches 0.003 kPa instead of 0 kPa as predicted by the low concentration model.

H_2S with residual CO_2 in 20.2 wt. % DEA at 323.0 K

Measurements were made of eleven mixtures composed of hydrogen sulfide and carbon dioxide in 20.2 wt. % DEA at 323.0 K. Only hydrogen sulfide was added to the DEA solution, but a small amount of initial carbon dioxide accounted for β, or $[CO_2]/[DEA]$, ~0.0025. The solubility data are listed in Table 4 and shown together with literature data by Leibush and Shneerson (1950) and Lee et al. (1973) in Figure 14. These data are also displayed with other hydrogen sulfide data at different conditions in Figure 11.

Table 2. H_2S with $\beta \sim 0.0063$ in 20.3 wt. % DEA at 322.8 K

P_{H_2S}/kPa	H_2S/DEA Mole Ratio	P_{CO_2}/kPa	CO_2/DEA Mole Ratio
0	0	0.00125	0.00628
0	0	0.00140	0.00634
0	0	0.00163	0.00634
0	0	0.00179	0.00633
0.0097	0.00931	0.00190	0.00633
0.0348	0.01836	0.00297	0.00631
0.1078	0.03162	0.00427	0.00629
0.1778	0.04173	0.00517	0.00628
0.3165	0.05682	0.00662	0.00625

As shown in Figure 12 (Table 4), the hydrogen sulfide pressures of 0.06 kPa and below are linear with $Fn(H_2S)_D$, and the hydrogen sulfide pressure approaches 0 kPa as the loading approaches zero, within the experimental error, as predicted by the model.

Residual carbon dioxide is from the desorbing cell, seals, and tubing surfaces, and a small amount in the DEA, which was distilled to remove most of the original carbon dioxide and other ethanolamines. The carbon dioxide measurement precision of the FTIR method permits determination of residual carbon dioxide, which affects the solubility of hydrogen sulfide in the alkanolamines.

As shown in Figure 10 (Table 4), residual carbon dioxide pressures of 0.008 kPa and below are linear with $Fn(CO_2)_D$, as predicted by the model. Also, as the loading approaches zero, the carbon dioxide pressure approaches 0.1 Pa, which is 0 Pa within the experimental error.

The ratio of the carbon dioxide and hydrogen sulfide pressure, P_{CO_2}/P_{H_2S}, is shown for this system in Figure 13 (Table 4). The curvature is similar to the curvature for the system with higher initial β (Table 2), as discussed earlier, and is

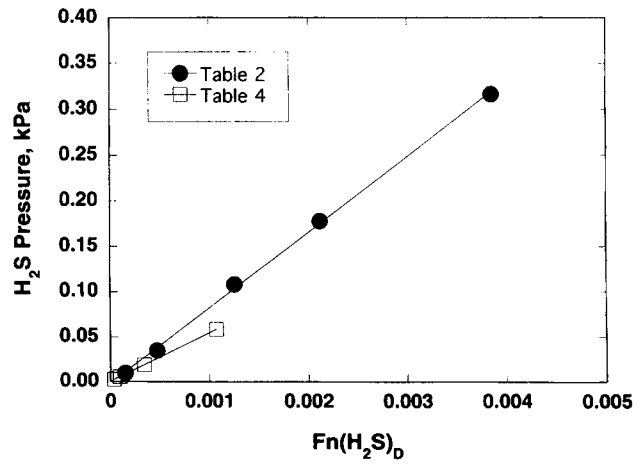

Figure 12. Low-pressure H_2S in 20 wt. % DEA at 323 K.

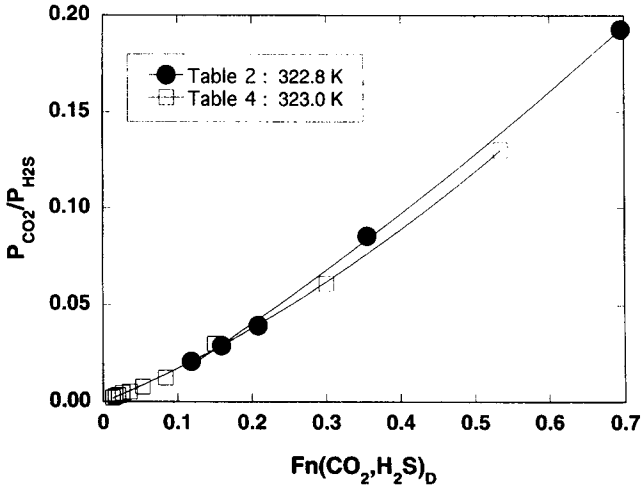

Figure 13. CO_2, H_2S pressure ratio in 20 wt. % DEA.

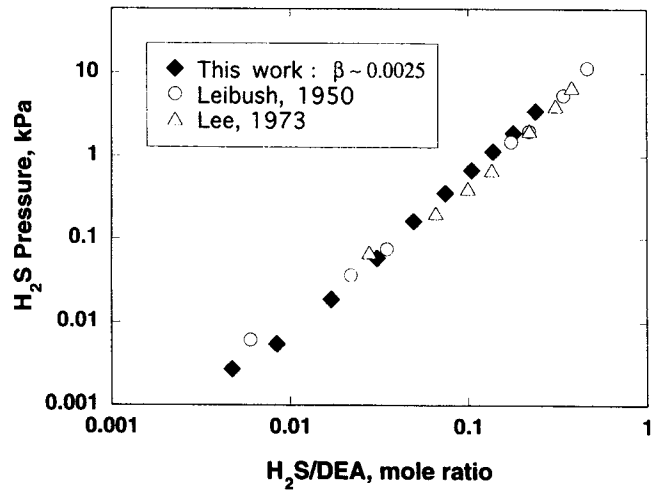

Figure 14. H_2S solubility in 20.2 wt. % DEA at 323.0 K.

inconsistent with the low concentration model, which predicts a linear dependence.

The hydrogen sulfide loading values for this system with an initial $\beta \sim 0.0025$ are shown in Figure 11 together with values (from Table 2) for hydrogen sulfide in 20.3 wt. % DEA with an initial $\beta \sim 0.0063$. The expected effect of CO_2 on the H_2S solubility at low concentrations of H_2S is demonstrated with higher H_2S pressures at a given α measured for the higher CO_2 loading condition.

H_2S with residual CO_2 in 20.2 wt. % DEA at 313.2 K

After lowering the temperature of the DEA sample discussed just now from 323.0 to 313.2 K, VLE measurements were made of hydrogen sulfide and residual carbon dioxide for various amounts of added H_2S. The VLE results for this system are listed in Table 5 and compared with literature data by Lal et al. (1985) and Lawson and Garst (1976) in Figure 15. These data are also displayed with other hydrogen sulfide data at different conditions in Figure 11 (Table 5).

Residual carbon dioxide pressures below 0.01 kPa are shown to be linear with $Fn(CO_2)_D$ in Figure 10 (Table 5), and the carbon dioxide pressure approaches ~ -0.6 Pa, within the experimental error, as the loading approaches zero.

CO_2 with $\alpha \sim 0.408$ in 20.2 wt. % DEA at 313.2 K

Measurements were made of carbon dioxide and hydrogen sulfide in the 20.2 wt. % DEA system, discussed just now, as amounts of CO_2 were added. Data from measurements of four VLE compositions of H_2S and CO_2 in the DEA solution are listed in Table 6. The CO_2 solubility for these four compositions is shown in Figure 9, which also shows the rise in CO_2 pressure (Table 5) when H_2S was added in the previous experiment. In these studies, the mutual effects of CO_2 and H_2S on their solubility in the DEA system were measured and demonstrated.

Carbon dioxide pressures of 0.2 kPa and below are linear with $Fn(CO_2)$. These pressures are probably outside the low-concentration range of the model, especially with the high initial loading of hydrogen sulfide. As a result, the limiting carbon dioxide pressure is ~ 0.7 Pa instead of 0 Pa.

Table 3. CO_2 with $\alpha \sim 0.056$ in 20.3 wt. % DEA at 322.8 K

P_{H_2S}/kPa	H_2S/DEA Mole Ratio	P_{CO_2}/kPa	CO_2/DEA Mole Ratio
0.3330	0.05637	0.0199	0.01431
0.3503	0.05581	0.0339	0.02259
0.4027	0.05524	0.0563	0.03419
0.4392	0.05441	0.0951	0.05056
0.5144	0.05279	0.1959	0.08302
0.5916	0.05071	0.3390	0.1156

Conclusions

The feasibility of FTIR measurements of acid gases in aqueous solutions of alkanolamines was demonstrated. Its advantages include measurements of the vapor and liquid VLE components without disturbing the system equilibrium or removing them from the apparatus for remote analysis.

Sulfur compounds are strongly adsorbing on surfaces, and methods that require external sampling are subject to shifts in composition caused by unequilibrated surfaces. The effects of adsorption on sample measurements increase at low acid gas concentrations. In the closed system of the FTIR apparatus, however, the sample is equilibrated with all surfaces before and during measurements. Residual carbon dioxide, which affects the VLE data of other acid gas species, can be determined in low-concentration mixtures.

Table 4. H_2S with Residual CO_2 in 20.2 wt. % DEA at 323.0 K

P_{H_2S}/kPa	H_2S/DEA Mole Ratio	P_{CO_2}/kPa	CO_2/DEA Mole Ratio
0	0	0.00029	0.002501
0.0028	0.00472	0.00036	0.002500
0.0063	0.00844	0.00034	0.002500
0.0189	0.01703	0.00057	0.002495
0.0586	0.03089	0.00072	0.002492
0.1620	0.04953	0.00126	0.002482
0.3578	0.07458	0.00186	0.002471
0.6819	0.1053	0.00303	0.002448
1.151	0.1383	0.00386	0.002431
1.923	0.1802	0.00517	0.002404
3.532	0.2404	0.00758	0.002356

Table 5. H_2S with Residual CO_2 in 20.2 wt. % DEA at 313.2 K

P_{H_2S}/kPa	H_2S/DEA Mole Ratio	P_{CO_2}/kPa	CO_2/DEA Mole Ratio
2.777	0.2588	0.00379	0.002431
3.622	0.2996	0.00517	0.002404
5.415	0.3556	0.00731	0.002360
7.739	0.4081	0.00979	0.002307

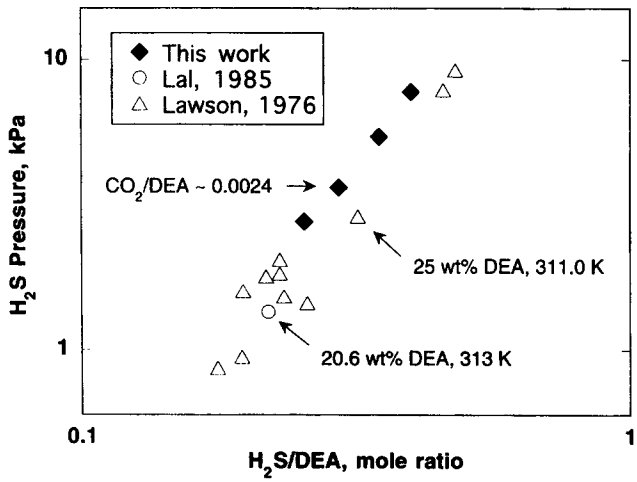

Figure 15. H_2S solubility in 20.2 wt. % DEA at 313.2 K.

In systems with either carbon dioxide or hydrogen sulfide or both of these acid gases, carbon dioxide and hydrogen sulfide partial pressures were represented well at low concentrations and were linear with respect to the functions $Fn(CO_2)$ and $Fn(H_2S)$, as predicted by the low-concentration model. The solubility of carbon dioxide and hydrogen sulfide in aqueous solutions of the alkanolamines was affected by the presence of the other acid gas in the manner predicted by this equilibrium model.

Perhaps the result of the model approximations, P_{CO_2}/P_{H_2S} plotted against $Fn(CO_2,H_2S)$ was systematically quadratic and concave upward instead of linear as predicted by the low-concentration model.

In addition, the FTIR method is capable of measuring the ionic reaction products of acid gases with ethanolamines, such as protonated alkanolamine, carbamate, bicarbonate, and bisulfide. The capability to measure these species can be expecially useful in developing and testing detailed reaction models for these systems.

Table 6. CO_2 with $\alpha \sim 0.408$ in 20.2 wt. % DEA at 313.2 K

P_{H_2S}/kPa	H_2S/DEA Mole Ratio	P_{CO_2}/kPa	CO_2/DEA Mole Ratio
7.739	0.4081	0.00979	0.002307
7.810	0.4057	0.0345	0.008121
8.246	0.3911	0.1926	0.03786
9.467	0.3544	0.8905	0.1079

Acknowledgment

The financial sponsors for this project include the Center for Energy and Mineral Resources at Texas A&M University, Amoco, Texaco Chemical, U.S. Department of Energy, Gas Research Institute, and the Gas Processors Association.

The apparatus used in this project was originally built by Richard E. Frazier in partial fulfillment of the requirements for a Ph.D. in Chemical Engineering at Texas A&M University, College Station (1993).

Notation

$A^0 = RR'R''N$
$A^+ = RR'R''NH^+$, protonated alkanolamine
A = total amine species
AU = absorbance unit
$C^- = RR'NCOO^-$ = carbamate
$[(CH_2)_2 - OH]_2NH$ = DEA
$RR'R''N$ = alkanolamine
$\alpha = [H_2S]/[DEA]$, mole ratio
$\beta = [CO_2]/[DEA]$, mole ratio

Literature Cited

Astarita, G., and D. W. Savage, "Simultaneous Absorption with Reversible Instantaneous Chemical Reaction," *Chem. Eng. Sci.*, **37**(5), 677 (1982).

Austgen, D. M., G. T. Rochelle, X. Peng, and C.-C. Chen, "Model of Vapor-Liquid Equilibria for Aqueous Acid Gas-Alkanolamine Systems Using the Electrolyte-NRTL Equation," *Ind. Eng. Chem. Res.*, **28**(7), 1060 (1989).

Davis, R. A., R. E. Menéndez, and O. C. Sandall, "Physical, Thermodynamic, and Transport Properties for Carbon Dioxide and Nitrous Oxide in Solutions of Diethanolamine or Di-2-propanolamine in Polyethylene Glycol," *J. Chem. Eng. Data*, **38**, 119 (1993).

Frazier, R. E., "Acid Gas–Diethanolamine Vapor–Liquid Equilibrium Data by Fourier Transform Infrared Spectroscopy," PhD Diss., Texas A&M Univ., College Station (1993).

Issacs, E. E., F. D. Otto, and A. E. Mather, "Solubility of Mixtures of H_2S and CO_2 in a Monoethanolamine Solution at Low Partial Pressures," *J. Chem. Eng. Data*, **25**, 118 (1980).

Lal, D., F. D. Otto, and A. E. Mather, "The Solubility of H_2S and CO_2 in a Diethanolamine Solution at Low Partial Pressures," *Can. J. Chem. Eng.*, **63**(4), 681 (1985).

Lawson, J. D., and A. W. Garst, "Gas Sweetening Data: Equilibrium Solubility of Hydrogen Sulfide and Carbon Dioxide in Aqueous Monoethanolamine and Aqueous Diethanolamine Solutions," *J. Chem. Eng. Data*, **21**, 20 (1976); also, correction, *J. Chem. Eng. Data*, **41**, 1210 (1996).

Lee, J. I., F. D. Otto, and A. E. Mather, "The Solubility of Mixtures of Carbon Dioxide and Hydrogen Sulfide in Aqueous Diethanolamine Solutions," *Can. J. Chem. Eng.*, **52**, 125 (1974).

Lee, J. I., F. D. Otto, and A. E. Mather, "Partial Pressures of Hydrogen Sulfide over Aqueous Diethanolamine Solutions," *J. Chem. Eng. Data*, **18**, 420 (1973).

Leibush, A. G., and A. L. Shneerson, "The Absorption of Hydrogen Sulfide and of its Mixtures with Carbon Dioxide by Ethanolamines," *Zh. Prikl. Khim.*, **23**, 145 (1950).

Murzin, V. I., and I. L. Leites, "Partial Pressure of Carbon Dioxide over Dilute Solutions of Aqueous Diethanolamine," *Zh. Fiz. Khim.*, **45**, 2642 (1971).

Sartori, G., and D. W. Savage, "Sterically Hindered Amines for CO_2 Removal from Gases," *Ind. Eng. Chem. Fundam.*, **22**, 239 (1983).

Stewart, E. J., and R. A. Lanning, "Reduce Amine Plant Solvent Losses: 1," *Hydroc. Proc.*, 67 (1994).

Thorne, A. P., *Spectrophysics*, Chapman & Hall, New York (1988).

White, J. U., "Long Optical Paths of Large Aperture," *J. Opt. Soc. Amer.*, **32**, 285 (1942).

Manuscript received Aug. 1, 1996, and revision received Aug. 7, 1997.